

Tail-structure regulated phase behaviors of a lipid bilayer

Wenwen Li(李文文), Zhao Lin(林召), Bing Yuan(元冰), and Kai Yang(杨恺)

Citation: Chin. Phys. B, 2020, 29 (**12**): 128701. DOI: 10.1088/1674-1056/abad20
Journal homepage: http://cpb.iphy.ac.cn; http://iopscience.iop.org/cpb

What follows is a list of articles you may be interested in

Effect of C_{60} nanoparticles on elasticity of small unilamellar vesicles composed of DPPC bilayers

Tanlin Wei(魏坦琳), Lei Zhang(张蕾), Yong Zhang(张勇)
Chin. Phys. B, 2020, 29 (**4**): 048702. DOI: 10.1088/1674-1056/ab7d9f

Effects of Mg^{2+} on the binding of the CREB/CRE complex: Full-atom molecular dynamics simulations

Song Mao(毛松), Shuai Wang(王帅), Haiyou Deng(邓海游), Ming Yi(易鸣)
Chin. Phys. B, 2019, 28 (**7**): 078701. DOI: 10.1088/1674-1056/28/7/078701

Protein-membrane interactions investigated with surface-induced fluorescence attenuation

Li Ma(马丽), Ying Li(李颖), Ming Li(李明), Shuxin Hu(胡书新)
Chin. Phys. B, 2017, 26 (**12**): 128708. DOI: 10.1088/1674-1056/26/12/128708

Molecular dynamic simulation of the thermodynamic and kinetic properties of nucleotide base pair

Yu-Jie Wang(王宇杰), Zhen Wang(王珍), Yan-Li Wang(王晏莉), Wen-Bing Zhang(张文炳)
Chin. Phys. B, 2017, 26 (**12**): 128705. DOI: 10.1088/1674-1056/26/12/128705

Combined effects of headgroup charge and tail unsaturation of lipids on lateral organization and diffusion of lipids in model biomembranes

Xiao-Jie Chen(陈晓洁), Qing Liang(梁清)
Chin. Phys. B, 2017, 26 (**4**): 048701. DOI: 10.1088/1674-1056/26/4/048701

Tail-structure regulated phase behaviors of a lipid bilayer*

Wenwen Li(李文文)[1,†], Zhao Lin(林召)[1,2,†], Bing Yuan(元冰)[1,‡], and Kai Yang(杨恺)[1,§]

[1] *Center for Soft Condensed Matter Physics and Interdisciplinary Research & School of Physical Science and Technology, Soochow University, Suzhou* 215006, *China*

[2] *School of Optoelectronic Science and Engineering, Soochow University, Suzhou* 215006, *China*

(Received 1 June 2020; revised manuscript received 9 July 2020; accepted manuscript online 7 August 2020)

Lateral heterogeneity of a cell membrane, including the formation of lipid raft-like clusters and the inter-leaflet coupling of specific phase domains, is crucial for cellular functions such as membrane trafficking and transmembrane signaling. However, the wide diversity in lipid species and the consequent complexity in lipid–lipid interplays hinder our understanding of the underlying mechanism. In this work, with coarse-grained molecular dynamics simulations, the effect of lipid tail structures on the phase behavior of a model ternary lipid membrane was systematically explored. A serial of 27 lipid membrane systems consisting of saturated, unsaturated lipids, and cholesterol (Chol) molecules, at a fixed molar ratio of 4:4:2 while varying in lipid structures including tail length, unsaturation degree, and/or position of unsaturated atoms, were constructed. These structural factors were found to exert sophisticated influences on packing states of the constituent molecules, especially Chol, in a bilayer, and modulate the complicated entropy–enthalpy competition of the membrane system accordingly. Specifically, an appropriate difference in effective tail length and distinct feature of the tail ends between the saturated and unsaturated lipid compositions promised an enhanced phase separation of the membrane into the Chol-rich Lo and Chol-poor Ld phase domains, with a full inter-leaflet coupling of each domain. Our results provide insights into the lipid organizations and segregations of the cellular plasma membrane.

Keywords: molecular dynamic simulation, lipid bilayers, phase separation, inter-leaflet coupling

PACS: 87.10.Tf, 87.14.Cc, 87.16.D–, 87.15.A– **DOI:** 10.1088/1674-1056/abad20

1. Introduction

Cellular plasma membrane is one of the most important entities of a cell, which contains thousand types of lipid species and a large variety of membrane proteins,[1–3] and there are complicated interaction among membrane and other proteins.[4–7] The lateral heterogeneity of membranes featuring a variety of distinct subcompartments that differ in compositions and biophysical properties, or so-called lipid raft hypothesis, is believed to be crucial during many cellular processes including membrane trafficking, transmembrane signaling, and virus infection, as well as some potential biomedical treatments such as drug or gene delivery to cells.[8–15] Unfortunately, although much effort has been made, debate on the mechanism and physiological relevance of lipid raft still exists because of the extreme complexity of a real biological membrane system. Bilayer membranes with specified lipid compositions provide a convenient model to study such membrane organizations in a controlled manner.[16] For example, saturated lipids (entitled Satlipids) such as 18:0,18:0-phosphatidylcholine (DSPC) and cholesterol (Chol) drive the formation of functional importance, relatively ordered membrane regions that recruit other lipids and proteins, in which the constituent molecules pack together tightly with highly ordered acyl chains (*i.e.*, liquid-ordered phase, Lo).[8] In contrast, liquid-disordered phase (Ld) is rich in unsaturated lipids (entitled Unsatlipids) such like 18:1,18:1-PC (DOPC) with low chain-ordering while high diffusivity. These domains are present in both the outer and inner leaflets of a bilayer and are presumably coupled across leaflets to form platforms for executing cellular functions.[10]

The huge diversities in lipid species, as well as the resultant complexity in lipid–lipid interactions,[17] are major bottlenecks for the study of phase behavior of lipid membranes. It has been shown that tiny deviations in lipid structure would produce strong effects on organizations of the membrane. For example, Chol, which accounts for 30 mol%–50 mol% of lipid molecules, is a key component to trigger domain formation in a bilayer membrane.[18–20] Róg *et al.* found that removal of tiny methyl groups in the ring structure of Chol would change the tilting state of Chol molecules in bilayer and influence the Chol–lipid interactions; as a result, the ordering and condensing effects of Chol on lipid membranes,

*Project supported by the National Natural Science Foundation of China (Grant Nos. 21422404, 21774092, U1532108, 21728502, and U1932121), the Priority Academic Program Development (PAPD) of Jiangsu Higher Education Institutions. K Yang and B Yuan acknowledge the support of the Natural Science Foundation of Jiangsu Province of China (Grant Nos. BK20171207 and BK20171210). Z Lin thanks the support of Undergraduate Training Program for Innovation and Entrepreneurship of Soochow University, China (Grant No. 201810285023Z).

†These authors contributed equally to this work.

‡Corresponding author. E-mail: yuanbing@suda.edu.cn

§Corresponding author. E-mail: yangkai@suda.edu.cn

© 2020 Chinese Physical Society and IOP Publishing Ltd

which are important for the phase separation of a multicomponent lipid bilayer, are modulated accordingly.[21] Docosohexaenoic acid (DHA), a type of polyunsaturated fatty acid with six double bonds in the 22-carbon acyl chain, is vital for a wide variety of biological functions including brain development and visual acuity.[22,23] Pitman and coworkers found that DHA could promote the lateral segregation of biological membranes due to the low affinity between such polyunsaturated fatty acid and Chol.[24,25] Interestingly, an investigation with solid-state NMR, x-ray diffraction, and molecular dynamics (MD) simulations indicated that the loss of a single double bond in DHA would obviously change the lipid segregation state of membrane.[26] Recently, Goh *et al.* found a surprising nanoscopic-to-macroscopic transition of lipid phase domains in a four-component lipid mixture when 18:1,18:1-PC (DOPC) is replaced with 16:0,18:1-PC (POPC).[27] Such modulated phase behavior is originated from the structural difference in acyl chains between the nanodomain-inducing POPC and the macrodomain-inducing DOPC.[28] However, molecular mechanisms underlying the effect of lipid structure on phase behaviors of membranes are largely elusive and systematic investigations are still lacking.

Computer simulations are powerful to explore the molecular mechanism of membrane-related biological processes.[7,29–35] Especially, coarse-grained (CG) MD gives a unique view of phase separation of a multicomponent lipid bilayer. For example, by using the well-established MARTINI CG model,[36] spontaneous formation of lipids domains in both model membranes and biologically realistic plasma membranes are successfully achieved.[17,37–40] Moreover, MD technique is particularly convenient in building different membrane systems with varying lipid species and therefore is suitable for a systematic analysis in comparison of experimental methods.[41] In this work, a serial of 27 ternary membrane systems, consisting of Satlipids, Unsatlipids, and Chols, were constructed using CG MARTINI model. Influences from the lipid structures including tail length as well as number and position of the unsaturated bonds, on phase behaviors of the membrane were explored. It is found that all these structural factors exert sophisticated influences through changing the packing states of constituent molecules, especially Chols, in bilayer, and consequently cause complicated changes of entropy and enthalpy of the system. Specifically, an appropriate difference in effective tail length and the distinct feature of tail ends between Satlipids and Unsatlipids tend to facilitate well phase separation of the membrane, demonstrated as a reduced phase boundary length and an enhanced inter-leaflet registration degree of specific lipid domains.

2. Models and methods

2.1. Simulation models and system

All simulations are carried out by using GROMACS 5.1.2 with the MARTINI CG force field and the updated Chol parameters.[42] Ternary membrane systems consisting of Satlipids, Unsatlipids, and Chols with a fixed ratio of 4:4:2 while different lipid structures are constructed (Fig. 1). Satlipid and Unsatlipid have the same phosphatidylcholine (PC)-type head groups while different tail chains. For Satlipid ($N:0, N:0$-PC), it has two asymmetric tails and each consists of N hydrophobic MARTINI CG C1-type beads, representing methylene/methyl units. For Unsatlipid ($N':n$, $N':n$-PC), it has symmetric tails with a length of N'. To account for the polarizable nature of the double bonds in Unsatlipid tail, n slightly polar C4-type beads are applied,[43] while the location of these beads (d) could vary. Representatively, in this work a serial of 27 membrane systems with 3 types of Satlipids and 9 types of Unsatlipids with varying N, N', n, and d values are constructed (Fig. S1). Furthermore, in each membrane system, the two leaflets are symmetric in composition. Therefore, each membrane system can be represented with the parameters of $\{n, d, r = N'/N\}$. It is worth noting that, as reported by previous studies,[44] phase separation of a multicomponent lipid bilayer is a rather complicated behavior and many factors such as the ratios of lipid composition affect this process. In our simulations, a fixed ratio of 4:4:2 is chosen based on the ternary phase diagram for Satlipid, Unsatlipid, and Chol.[45] It has proved that under such a ratio, phase separation a ternary lipid bilayer could be well realized.[39,46] Moreover, it is also helpful for us to concentrate on the influence of lipid type, especially its tail structure, on the phase behavior of a lipid bilayer.

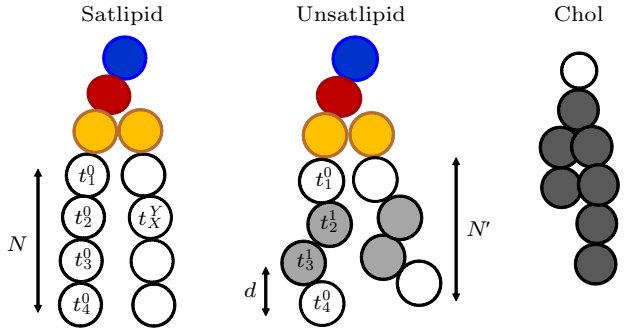


Fig. 1. Characterization of a ternary membrane system consisting of Satlipids, Unsatlipids, and Chols. The system is described with parameters of $\{n, d, r = N'/N\}$. n represents the number of C4-type beads (grey) in a Unsatlipid which indicates the unsaturation degree of the system. d refers to location of the last C4-type bead from the tail end as $d = N' - \mathrm{Max}(X|_{Y=1})$. N (N') refers to the total bead amount of the tail of a Satlipid (Unsatlipid). Each bead of the lipid molecule can be described with t_X^Y, where X and Y refer to the location ($X = 1, 2, \ldots$) and type (0 for C1-type (white) and 1 for C4-type (grey)) of the bead, respectively.

2.2. Simulation details

The bilayer is built by using insane script.[41] At initial state, the membrane components are randomly distributed in the membrane plane. After energy minimization and a short equilibrium process, the system is simulated in the *NPT* ensemble for at least 10 μs and three independent runs are performed for each membrane system to ensure the computational convergence and consistency.

The simulations are carried out under the Verlet scheme with a time step of 20 fs. The system temperature is set to be 300 K, which is controlled with the velocity-rescale method[47] with a time constant of 1 ps. Semi-isotropic pressure coupling is applied throughout the simulations, by using a Berendsen barostat[48] during the equilibrium process; then, shifted to a Parrinello–Rahman barostat[49] with the compressibility of 3×10^{-4} bar^{-1} (1 bar = 10^5 Pa) and the reference pressure of 1 bar. Van der Waals interactions are cut off at 1.1 nm and shifted to zero starting at 0 and 1.1 nm; meanwhile, the electrostatic interactions are calculated with the efficient reaction field method with a dielectric constant of 15. The neighbor list is updated every 10 steps with a neighbor list cutoff range of 1.1 nm. The periodic boundary conditions are applied in all three directions. In addition, time evolution of the characteristic parameters, including interaction energy, pressure and temperature of the membrane system, reaches equilibrium quickly ($<$ 300 ns) and keeps constant throughout the following simulations (Fig. S2). This suggests a good stability of our membrane system under the applied simulation conditions.

2.3. Data analysis

The phase separation behavior of a lipid bilayer membrane could be described by the formation of lipid phase domains in each leaflet and the coupling of domains between the two leaflets. The lipid phase in a leaflet is determined by analyzing the local lipid compositions with a Voronoi tessellation scheme.[50] In brief, the Voronoi tessellation is performed firstly based on the mass center of all lipids in the leaflet. Then, according to the surrounding molecules, the lipid of interest could be classified as a certain phase, Lo or Ld: if the adjacent environment of the molecule is enriched in Satlipid or Chol, it is determined as Lo phase; otherwise, it is considered in the Ld phase (Fig. 2).[45] Therefore, based on this scheme, the leaflet finally consists of two types of Voronoi cells: Lo or Ld (Fig. 2). If two neighbor cells belong to different phases, the shared Voronoi edge is considered as a phase boundary, and the sum of the lengths of all boundaries (their projections in the *xy* plane are normally used instead) is taken as the length of phase boundary of a leaflet. Thus, the degree of phase separation could be described by the length of phase boundary (L). For a well-separated membrane, L is smaller, while for a membrane with many mosaic domains, L is larger.

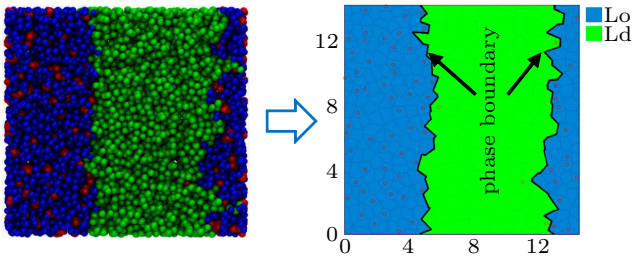


Fig. 2. Voronoi tessellation of one leaflet (right, gray lattice) of a lipid bilayer (left) and the Lo/Ld phase determination. The phase boundary is highlighted by thick black lines.

The coupling of phase domains between the two leaflets is determined by registration degree of the domains. A perfect registration means the same phase domains align exactly across the bilayer, while an anti-registration indicates the phase domains in the two leaflets are totally misaligned (Fig. 3(a)). In order to give a quantitative description of the registration degree, correlation $C(k,l) = \iint_{-\infty}^{+\infty} P(x,y)\,P'(x-k,y-l)\,\mathrm{d}x\mathrm{d}y$, in which $P(x,y)$ is the location of a phase domain in one leaflet, P' is the location of the same phase in the opposing leaflet, and k, l represent the displacement in X and Y directions, is used. Thus, the profile of $C(k,l)$, especially its 1D projected curve $C(R)$ (R is the distance between the domains), could clearly provide the degree of domain registration (Fig. 3(b)): in the case of perfect registration, the peak of $C(R=0)$ appears; while in the case of anti-registration, such peak is displaced.

As the most important driving molecule for phase separation of a lipid bilayer,[51] the spatial distribution and orientation of Chol are specifically analyzed. As done by Weiner *et al.*,[44] the Chol molecules are classified into two types according to their locations, including those at the midplane layer and those in both leaflets of a membrane. Here, the midplane Chol is defined as the molecules whose hydroxyl bead (ROH) is more than 1.4 nm away from the nearest phosphate bead of lipid (PO_4).[44] The orientation of each Chol molecule could be calculated accordingly.

The effective tail length of a lipid is determined as the Euclidean distance between the Na-type bead (referring to GL2 group) at the head and the last bead at tail end of the lipid, and averaged between the two tails (Fig. S3). The output value of a lipid component in a membrane system is calculated based on all the lipid molecules throughout the last 1-μs simulations, and shown as mean ±SD.

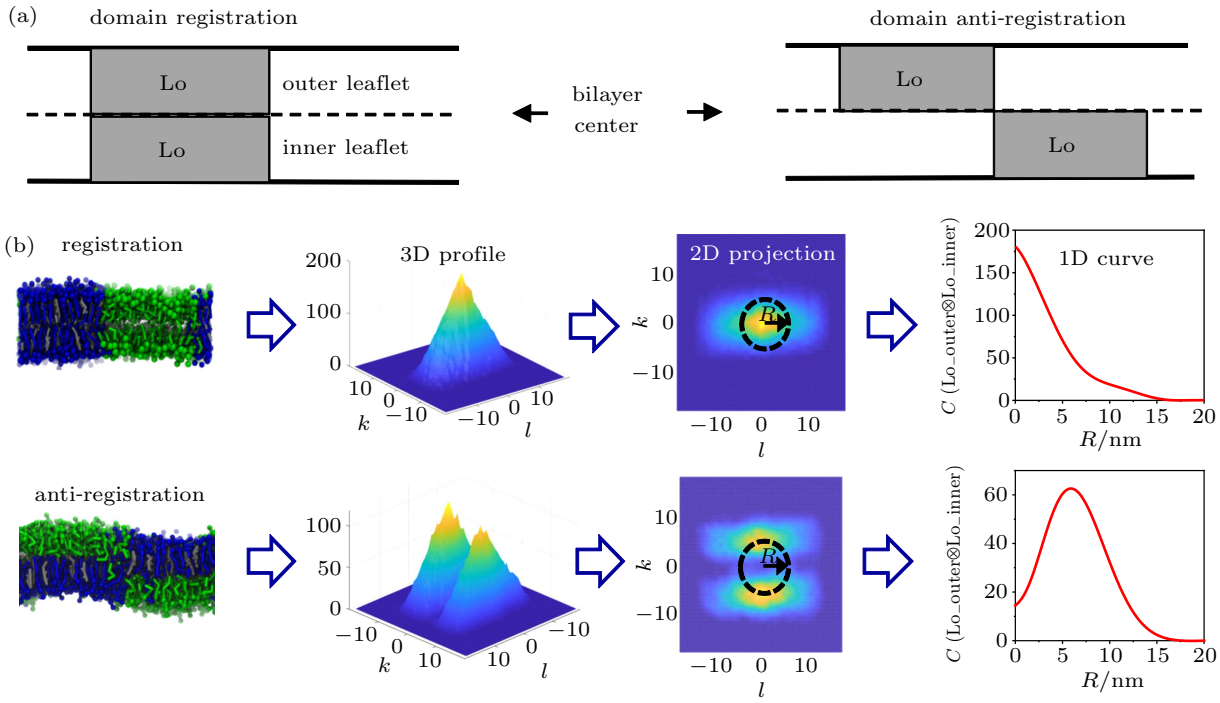


Fig. 3. Sketches of (a) phase domain registration and (b) calculation of the correlation function $C(k,l)$.

3. Results and discussion

3.1. Phase behavior of membranes with different lipid tail structures

The influence of lipid tail structure, as characterized with the parameters of $\{n,d,N'/N\}$, on membrane organizations was firstly examined. For simplification, a group of ternary membrane systems with varying values of n, d, and N'/N ratio, while other parameters being fixed, were constructed. The simulation results of three typical membrane systems are shown in Fig. 4. For the membrane with $\{2,1,4/4\}$ (*i.e.*, $n=2$, $d=1$, and $N'=N=4$), referring to the frequently-used 16:0, 16:0-PC (DPPC)/ 18:2, 18:2-PC (DUPC)/Chol system in simulations,[44,52] phase separation occurs rapidly, although with rough phase boundary (Fig. 4, left column). Based on this, an enhanced unsaturation degree, *e.g.*, the number of unsaturated beads being increased from 2 to 3 (*i.e.*, $\{3,0,4/4\}$), would further improve the phase separation phenomenon with much clearer boundaries. Moreover, the domains (*e.g.*, Lo domain in blue) in the two leaflets display an almost full registration (Fig. 4, middle column). However, if we cut the tail of the saturated lipids to only half of the unsaturated ones (*i.e.*, $\{2,1,4/2\}$), the phase separation would be greatly restricted (Fig. 4, right column). Therefore, these results clearly demonstrate that the diversity in lipid tail structure has strong influences on organizations of a lipid bilayer membrane.

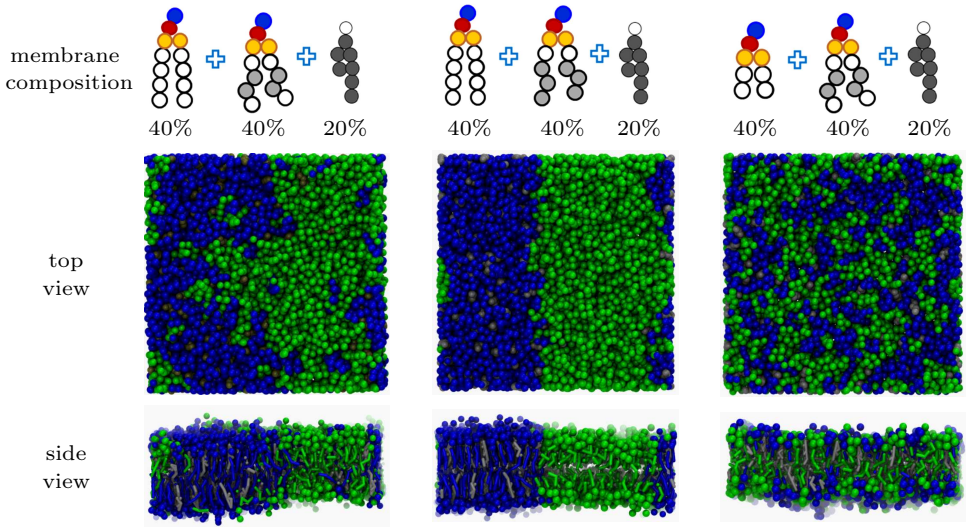


Fig. 4. Snapshots showing the effect of lipid tail structure on membrane organizations. From left to right, the membrane systems are $\{2,1,4/4\}$, $\{3,0,4/4\}$, and $\{2,1,4/2\}$, respectively. Composition and structure of the lipids in each system are shown on the top. All snapshots are obtained at $t=10$ μs.

3.2. Lipid-structure determined phase separation

To quantitatively describe such influence, time evolution of the boundary length, L, between adjacent phase domains was acquired. For all the membrane systems under investigation, L became constant (with small fluctuations) quickly with time, indicating all the systems were stable. Figures 5 and S4 show the L distributions of systems with various lipid structures, in which all the structural parameters including not only tail length but also amount and location of the unsaturated beads play important roles. As a direct indicator of the phase separation degree, a smaller L refers to an enhanced phase separation effect while a larger L corresponds to a more blurred boundary. Note that, in parallel runs, similar phase separation phenomena are observed (Fig. S5). It is observed that, for the membranes with the same lipid tail length and unsaturation degree, the location of the unsaturated beads determines, as a decreased d value (with double bonds being closer to the tail end; *e.g.*, being changed from $d = 2$ to $d = 1$ or 0) would enhance the phase separation effect significantly (Figs. 5(a) and S6A). This indicates that the feature of tail ends plays key roles in determining the lipid's property. Based on this system, a shortened tail length of the Satlipid molecules, *e.g.*, from $N = 4$ to $N = 3$ or 2, would obviously disturb the phase separation behavior (Figs. 5(b) and S6A). However, if we further enhance the unsaturation degree of the membrane, *e.g.*, increase the unsaturated bead number from $n = 2$ to $n = 3$ or 4, the phase separation ability of the membrane would be recovered again (Figs. 5(c) and S6A). This observation is consistent with the usual consideration that, with an increased unsaturation degree, a ternary lipid bilayer becomes better phase separated.[53] In contrast, for the membrane systems consisting of Satlipids and Unsatlipids with the same tail length (for example, $N = N' = 4$), the unsaturation degree would not influence anymore and the membrane always turns on good phase separation effect (Figs. 5(d) and S6A). These results demonstrate that the feature of tail ends plays dominant roles in determining lipid phase properties, *e.g.*, the coexistence of saturatedly-ended and unsaturatedly-ended lipids (with similar tail length) would lead to obvious phase separation behavior of a membrane.

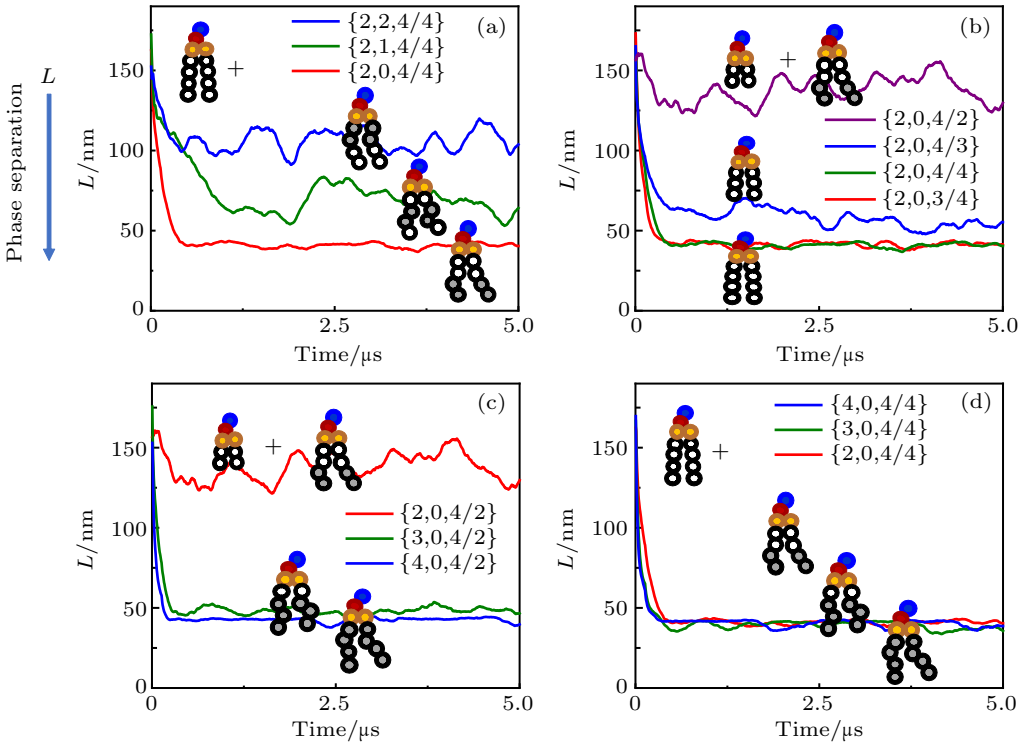


Fig. 5. Effects of lipid structure on the distribution of phase boundary length L. A smaller L value refers to a better phase separation effect.

3.3. Lipid-structure determined inter-leaflet phase registration

The inter-leaflet coupling of phase domains is also an important aspect of the phase behavior of lipid bilayer membranes. Here, the degree of phase domain registration was described with the correlation parameter $C(R)$ of Lo domains between the two leaflets (see Methods). It is observed that the lipid structure including tail length as well as amount and location of the unsaturated beads performs significant effects on $C(R)$ distribution. As shown in Figs. 6 and S7, the closer the unsaturated bead approaches tail end (demonstrated as a smaller d), the stronger the coupling occurs (as a larger $C(R = 0)$ value; Figs. 6(a) and S6B). Moreover, a shortened tail length of the Satlipids in comparison of the Unsatlipids (*i.e.*, a larger N'/N ratio) would weaken

the phase coupling effect (Figs. 6(b) and S6B). An increased unsaturation degree (*e.g.*, from $n = 2$ to $n = 3$ or $n = 4$) significantly improves the inter-leaflet coupling, especially when the Satlipids and Unsatlipids have similar tail length (Figs. 6(c), 6(d), and S6B). Such influences of lipid structure on C distribution coincide well with that on L, which confirms the coupling effect among different structural parameters of lipids on phase behavior of the membrane.

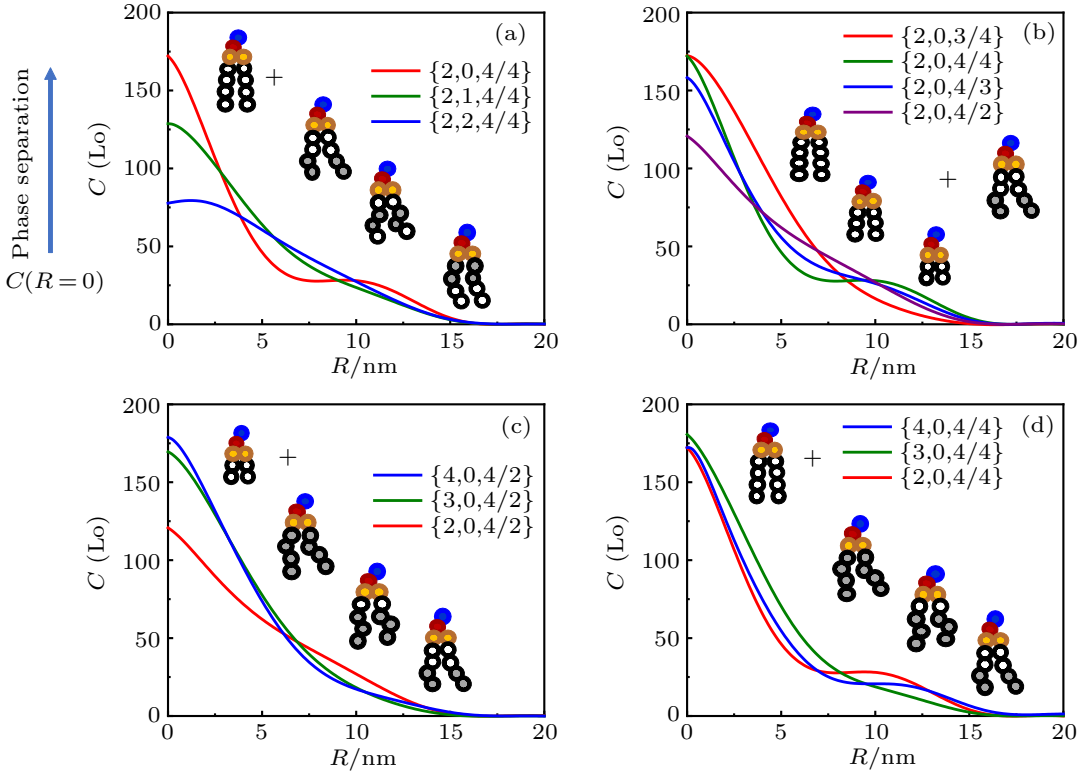


Fig. 6. Effects of n, d, and N'/N on the distribution of phase-registration degree $C(R)$. A larger $C(R = 0)$ value refers to a better phase separation effect.

3.4. Spatial distribution of Chol in the bilayer

As a key component for the formation of lipid rafts or membrane domains,[21,54,55] the distribution of Chol molecules in bilayer is expected to play crucial roles in determining properties of the membrane.[44] Here we analyzed the location and orientation of Chols, as well as their correlation with specific lipid species in the two leaflets. As representatively shown in Figs. 7(a) and 7(b), for the $\{2,0,4/4\}$ system as a well phase-separated membrane (in red), high and narrow peaks are observed in the distribution profiles of both z-position and orientation angle of Chol in bilayer, indicating that the Chol molecules locate neatly in the two leaflets. However, for the $\{2,0,4/2\}$ system as a homogeneous membrane without phase separation, the density distribution peaks of Chol become lower and broader; meanwhile, the Chol molecules become tilted rather than aligning upright in the membrane, and some Chol molecules tend to lie at the mid-plane region. Moreover, correlation analysis shows that, these mid-plane Chols turn on balanced correlation with the Satlipids and Unsatlipids (Fig. 7(c)). In contrast, Chols of the partly separated system (*e.g.*, $\{2,1,4/4\}$) demonstrates a much higher correlation with the Unsatlipids in comparison with the Satlipids. (For the well phase-separated system $\{2,0,4/4\}$, the correlation is quite low due to the little amount of mid-plane Chols.) These results demonstrate that the distribution of Chol molecules inside a bilayer especially those in the mid-plane layer, including their packing and orientation states, is closely related with tail structures of lipid components as well as phase separation behavior of the membrane.

3.5. Enthalpy-entropy competition in phase separation of the membrane

The lipid-structure dependent distribution of Chol in bilayer suggests its correlation with phase behavior of the membrane. For example, for the $\{2,0,4/4\}$ system consisting of Satlipids and Unsatlipids with tails of similar effective length (Table 1), most Chol molecules tend to stand upright aside Satlipids in the two leaflets due to the affinity between their rigid sterol chains and the saturated lipid tails, which drives the formation of Chol-rich Lo domains[51] being expelled away by the diffusive Unsatlipids (Fig. 8(a)). This also explains why the phase-separation degree of a multicomponent lipid bilayer further increases with an enhanced unsaturation degree of the Unsatlipids (*i.e.*, a larger n value). However, a larger d value decreases the effective tail length of the Unsatlipids

(*e.g.*, from $\{2,0,4/4\}$ to $\{2,1,4/4\}$). The resultant space between leaflets[56] as well as the saturated feature of their tail ends (Table S1) accommodate more mid-plane Chols, which weakens the driving force for Lo domain formation and blurs the boundary between different domains (Fig. 8(f)). At the same time, the appearance of mid-plane Chol decreases the inter-leaflet tension,[37] and thus reduces the registration degree of the phase domains between leaflets.

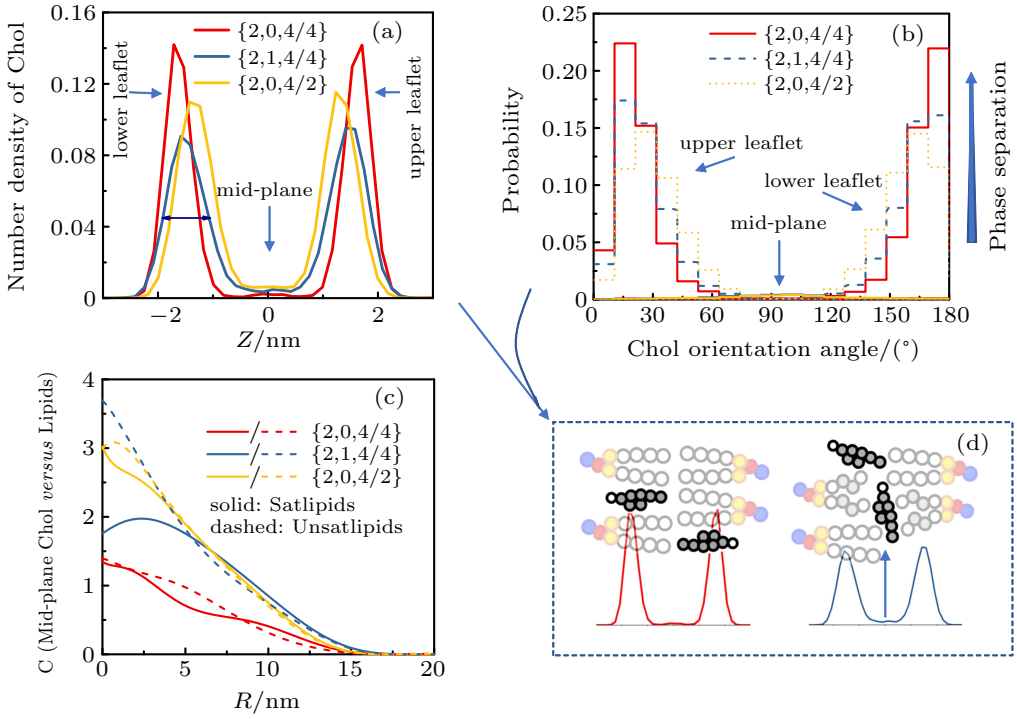


Fig. 7. Distribution of Chol in typical membrane system. (a) Number density distribution of Chol along Z direction. (b) Orientation distribution of Chol. Cartoons represent two typical types of Chol distribution as being upright in the leaflets or lying in the mid-plane as obtained from panels (a) and (b). (c) Correlations between mid-plane Chols and Satlipids or Unsatlipids in the leaflets.

On the other hand, a larger N'/N ratio also influences due to the arisen gap between the effective tail lengths of Satlipids and Unsatlipids (*e.g.*, from $\{2,0,4/4\}$ to $\{2,0,4/2\}$; Table 1). In this situation, the shorter Satlipids in one leaflet have to align to the longer Unsatlipids in the opposed leaflet to avoid the occurrence of large line tension caused by the hydrophobic mismatch at the boundary between Satlipid and Unsatlipid domains (Fig. 8(d)).[39,57] Meanwhile, many Chol molecules move to and distribute evenly in the mid-plane layer to further weaken the inter-leaflet tension, which consequently restricts the phase separation behavior. With a much decreased N'/N ratio, similar phenomenon is also observed (*e.g.*, $\{3,0,3/4\}$; Figs. 8(e) and S8).

The unsaturated-bead number (*i.e.*, n) also influences the effective tail length of lipids, the effect of which is coupled with the N'/N ratio. For example, the gap between effective tail length of Satlipids and Unsatlipids in the $\{2,0,4/2\}$ system induces anti-registration of lipid domains between the two leaflets (Fig. 8(d)). However, an increased n value narrows the gap (*e.g.*, $\{4,0,4/2\}$; Table 1), which consequently weakens the anti-registration effect and facilitates the phase separation behavior (Fig. 8(c)).

In brief, it is found by our simulations that the distribution of Chol molecules in membrane is determined by tail structure of the lipids. Such distribution is a result of enthalpy-entropy competition of the system (as representatively shown in Fig. S9), which further affects phase behavior of the membrane. In general, there is strong affinity between Chols and Satlipid tails (Table S1). Thus, most Chol molecules tend to stay aside Satlipids once the effective tail length of the Satlipids is long enough, *i.e.*, being comparative with or longer than that of Unsatlipids. Such tendency will further induce formation of Chol-rich Lo domains and facilitates well phase separation of the membrane (Table 1, Indexes 1–3 and Figs. 8(a)–8(c)). However, when the effective tail length of Satlipids is much larger than, or especially shorter than that of Unsatlipids, the entropic changes become dominate. In this case, the available space between leaflets becomes large enough to accommodate more mid-plane Chol molecules. The inserted Chols further disturb the inter-leaflet registration and in turn decrease the phase separation degree of the membrane (Table 1, indexes 4 and 5 and Figs. 8(d)–8(e)). In addition, feature of the tail ends also plays roles. For example, if we move the unsaturated beads from the end to middle of the tail (*e.g.*, from $\{2,0,4/4\}$ to $\{2,1,4/4\}$), the amount of mid-plane Chols will increase, leading to blurring of the domain boundary (Table 1, indexes 1 and 6; Fig. 8(f)).

Table 1. Effective tail lengths of lipids in various membrane systems.

Index	Membrane system	Lipid tail length l/nm			
		Satlipid	Unsatlipid	Δl^*/nm	Phase separation
1	{2,0,4/4}	1.62 ± 13	1.41 ± 22	0.21	√
2	{2,0,3/4}	1.61 ± 13	1.04 ± 18	0.57	√
3	{4,0,4/2}	0.85 ± 08	1.10 ± 27	–0.25	√
4	{2,0,4/2}	0.85 ± 08	1.41 ± 20	–0.56	×
5	{3,0,3/4}	1.61±15	0.92 ± 20	0.69	×
6	{2,1,4/4}	1.60 ± 13	1.31 ± 26	–	×

*Difference in effective tail length between Satlipids and Unsatlipids.

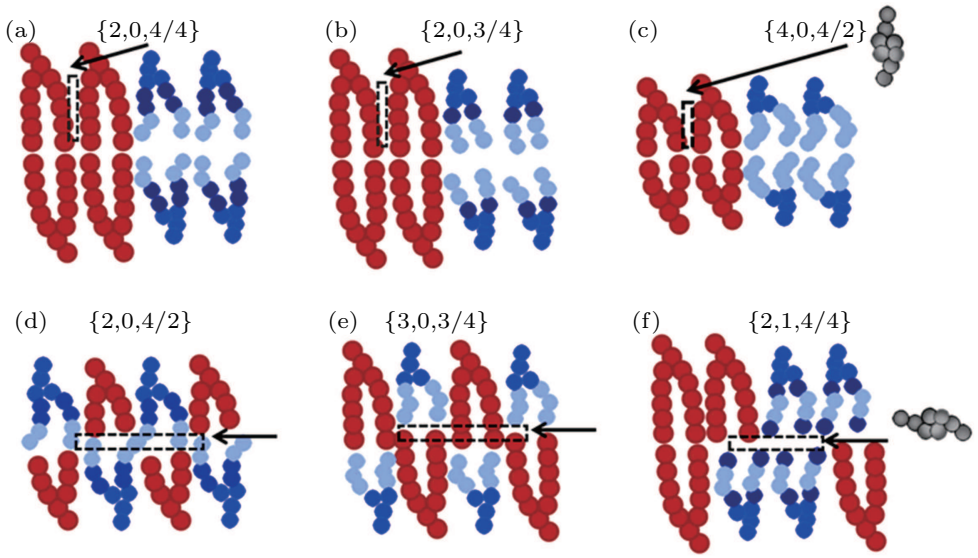


Fig. 8. Sketches of lipid-structure influence on Chol distribution and phase behaviors of lipid bilayers. Red: Satlipid; blue: Unsatlipid; light blue: Unsaturated tail bead; dark blue: saturated tail bead. Dashed box indicates the possible location of Chol.

4. Conclusion

In summary, it is demonstrated by our CG MD simulations that the diversity in lipid tail structure strongly affects the phase behavior of a bilayer membrane. Especially, factors like the difference in effective tail length between the saturated and unsaturated lipids as well as the position of double bonds in the unsaturated lipid tails, play key roles. In contrast, influence of the absolute value of tail length or unsaturation degree seems inconclusive. Moreover, the packing states of lipids especially the spatial distribution of Chol molecules in bilayer, which are affected by lipid tail structure due to the entropy–enthalpy competition of the membrane system, play significant roles in the formation of Lo and Ld phase domains and their inter-leaflet registration. Our findings provide insights into the phase behavior of bilayer membranes consisting of various lipid species, and are helpful for understanding the complicated organization manners of real plasma membranes and some related biological functions such as signal transition.

References

[1] Singer S J and Nicolson G L 1972 *Science* **175** 720
[2] Harayama T and Riezman H 2018 *Nat. Rev. Mol. Cell Biol.* **19** 281
[3] Yang Y, Lee M and Fairn G D 2018 *J. Biol. Chem.* **293** 6230
[4] Ma L, Li Y, Li M and Hu S 2017 *Chin. Phys. B* **26** 128708
[5] Xu C, Ma W, Wang K, He K, Chen Z, Liu J, Yang K and Yuan B 2020 *J. Phys. Chem. Lett.* **11** 4834
[6] Cheng X, Zhao L, Kai Y and Bing Y 2020 *Acta Phys. Sin.* **69** 108701 (in Chinese)
[7] Deng Z, Lu X, Xu C, Yuan B and Yang K 2020 *Soft Matter* **16** 3498
[8] Simons K and Ikonen E 1997 *Nature* **387** 569
[9] Sezgin E, Levental I, Mayor S and Eggeling C 2017 *Nat. Rev. Mol. Cell Bio.* **18** 361
[10] Lingwood D and Simons K 2010 *Science* **327** 46
[11] Liu J J, Chang Q, Bao M M, Yuan B, Yang K and Ma Y Q 2017 *Chin. Phys. B* **26** 098102
[12] Ding H, Li J, Chen N, Hu X, Yang X, Guo L, Li Q, Zuo X, Wang L, Ma Y and Fan C 2018 *ACS Cent. Sci.* **4** 1344
[13] Yang K and Ma Y Q 2010 *Nat. Nanotechnol.* **5** 579
[14] Lu X, Xu P, Ding H M, Yu Y S, Huo D and Ma Y Q 2019 *Nat. Commun.* **10** 4520
[15] Li M, Ding H, Lin M, Yin F, Song L, Mao X, Li F, Ge Z, Wang L, Zuo X, Ma Y and Fan C 2019 *J. Am. Chem. Soc.* **141** 18910
[16] Bennett W F D and Tieleman D P 2013 *Biochim. Biophys. Acta* **1828** 1765
[17] Ingolfsson H I, Melo M N, Van Eerden F J, Arnarez C, Lopez C A, Wassenaar T A, Periole X, De Vries A H, Tieleman D P and Marrink S J 2014 *J. Am. Chem. Soc.* **136** 14554
[18] Van Meer G, Voelker D R and Feigenson G W 2008 *Nat. Rev. Mol. Cell Biol.* **9** 112
[19] Ackerman D G and Feigenson G W 2015 *Essays Biochem.* **57** 33
[20] Baumgart T, Hess S T and Webb W W 2003 *Nature* **425** 821
[21] Rog T, Pasenkiewiczgierula M, Vattulainen I and Karttunen M 2007 *Biophys. J.* **92** 3346

[22] Menkes J H, Alter M, Steigleder G K, Weakley D R and Sung J H 1962 *A sex-linked recessive disorder with retardation of growth, peculiar hair, and focal cerebral and cerebellar degeneration*, Pediatrics, 1962 May 29, pp. 764–79 PMID: 14472668

[23] Stillwell W and Wassall S R 2003 *Chem. Phys. Lipids* **126** 1

[24] Pitman M C, Suits F, Mackerell A D and Feller S E 2004 *Biochemistry* **43** 15318

[25] Konyakhina T M and Feigenson G W 2016 *Biochim. Biophys. Acta* **1858** 153

[26] Eldho N V, Feller S E, Tristramnagle S, Polozov I V and Gawrisch K 2003 *J. Am. Chem. Soc.* **125** 6409

[27] Goh S L, Amazon J J and Feigenson G W 2013 *Biophys. J.* **104** 853

[28] Konyakhina T M, Wu J, Mastroianni J D, Heberle F A and Feigenson G W 2013 *Biochim. Biophys. Acta* **1828** 2204

[29] Liu J, Xiao S, Li J, Yuan B, Yang K and Ma Y 2018 *Biochim. Biophys. Acta* **1860** 2234

[30] Lu X, Liu J, Gou L, Li J, Yuan B, Yang K and Ma Y 2019 *Adv. Healthc. Mater.* **8** 1801521

[31] Ding H, Tian W and Ma Y 2012 *ACS Nano* **6** 1230

[32] Deng Z, Li J, Yuan B and Yang K 2019 *Commun. Theor. Phys.* **71** 887

[33] Ji Q, Yuan B, Lu X, Yang K and Ma Y 2016 *Small* **12** 1140

[34] Lu X, Liu J, Gou L, Li J, Yuan B, Yang K and Ma Y 2019 *Adv. Healthc. Mater.* **8** 1801521

[35] Xiao S, Lu X, Gou L, Li J l, Ma Y, Liu J, Yang K and Yuan B 2019 *Carbon* **149** 248

[36] Marrink S J, De Vries, H A and Mark A E 2004 *J. Phys. Chem. B* **108** 750

[37] Risselada H J and Marrink S J 2008 *Proc. Natl. Acad. Sci. USA* **105** 17367

[38] Koldso H, Shorthouse D, Helie J and Sansom M S P 2014 *Plos. Comput. Biol.* **10** e1003911

[39] Fowler P W, Williamson J J, Sansom M S P and Olmsted P D 2016 *J. Am. Chem. Soc.* **138** 11633

[40] Yang K, Yang R, Tian X, He K, Filbrun S L, Fang N, Ma Y and Yuan B 2018 *Phys. Chem. Chem. Phys.* **20** 28241

[41] Wassenaar T A, Ingolfsson H I, Bockmann R A, Tieleman D P and Marrink S J 2015 *J. Chem. Theory Comput.* **11** 2144

[42] Melo M N, Ingolfsson H I and Marrink S J 2015 *J. Chem. Phys.* **143** 243152

[43] Marrink S J, Risselada H J, Yefimov S, Tieleman D P and De Vries A H 2007 *J. Phys. Chem. B* **111** 7812

[44] Weiner M D and Feigenson G W 2018 *J. Chem. Phys. B* **122** 8193

[45] Ackerman D G and Feigenson G W 2015 *J. Phys. Chem. B* **119** 4240

[46] Perlmutter J D and Sachs J N 2011 *J. Am. Chem. Soc.* **133** 6563

[47] Bussi G, Donadio D and Parrinello M 2007 *J. Chem. Phys.* **126** 014101

[48] Berendsen H J C, Postma J P M, Van Gunsteren W F, Dinola A and Haak J R 1984 *J. Chem. Phys.* **81** 3684

[49] Parrinello M and Rahman A 1981 *J. Appl. Phys.* **52** 7182

[50] Ting F 2006 *Comput. Simul.* **23** 89

[51] Bennett W F D, Shea J and Tieleman D P 2018 *Biophys. J.* **114** 2595

[52] Thallmair S, Ingolfsson H I and Marrink S J 2018 *J. Phys. Chem. Lett.* **9** 5527

[53] Davis R S, Kumar P B S, Sperotto M M and Laradji M 2013 *J. Chem. Phys. B* **117** 4072

[54] Berkowitz M L 2009 *Biochim. Biophys. Acta* **1788** 86

[55] Rog T, Pasenkiewiczgierula M, Vattulainen I and Karttunen M 2009 *Biochim. Biophys. Acta* **1788** 97

[56] Javanainen M and Martinez-Seara H 2019 *Phys. Chem. Chem. Phys.* **21** 11660

[57] Williamson J J and Olmsted P D 2015 *Biophys. J* **108** 1963